Bioresource Technology 360 (2022) 127627

Contents lists available at ScienceDirect

Bioresource Technology

journal homepage: www.elsevier.com/locate/biortech

Effect of polytetrafluoroethylene nanoplastics on combined inhibition of ciprofloxacin and bivalent copper on nitrogen removal, sludge activity and microbial community in sequencing batch reactor

Huan Yang, Yueyue Wang, Zichao Wang *, Shengyu Yuan, Changwei Niu, Yaohui Liu, Yun Gao, Yuhan Li, Dan Su, Youtao Song

College of Environment Science, Liaoning University, Shenyang, China

HIGHLIGHTS

- PTFE-NPs weaken the Cu(II) and CIP antagonism on sludge activities.
- Nitrifier was more alive to Cu(II) and CIP than denitrifier with or without PTFE-NPs.
- Adsorption of CIP and Cu(II) by PTFE-NPs was synergistic.
- PN level in EPS was decreased by PTFE-NPs at mixed Cu(II)/CIP.
- PTFE-NPs abated the binding of functional groups in PN and PS to mixed Cu (II)/CIP.

GRAPHICAL ABSTRACT

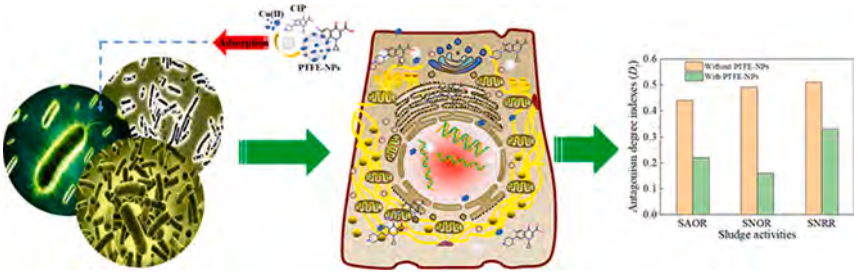

ARTICLE INFO

Keywords:
Nitrification
Denitrification
Antagonism degree index
Adsorption
Combined toxicity

ABSTRACT

The work aimed to explore effects of polytetrafluoroethylene nanoplastics on joint inhibitions of ciprofloxacin and bivalent copper on the nitrogen removal in a sequencing batch reactor and its potential mechanisms. The addition of bivalent copper and/or ciprofloxacin reduced the ammonia nitrogen elimination rate with or without polytetrafluoroethylene nanoplastics. Adsorption kinetics and thermodynamics showed the binary bivalent copper and ciprofloxacin promoted their adsorptions by polytetrafluoroethylene nanoplastics. Polytetrafluoroethylene nanoplastics enhanced combined toxicities of ciprofloxacin and bivalent copper to sludge activities and microbial community involved into nitrification and denitrification due to the adsorption of ciprofloxacin and bivalent copper by polytetrafluoroethylene nanoplastics. With or without polytetrafluoroethylene nanoplastics, bivalent copper and/or ciprofloxacin caused more obvious level changes of protein than polysaccharide. This study provides novel insights for understanding the effect of combined heavy metals and antibiotics on the performance in a sequencing batch reactor with the nanoplastics stress.

1. Introduction

Polytetrafluoroethylene (PTFE) has been used widely in industries, medicines and laboratories etc., and its fragments are found everywhere in natural environments (Karpenko et al., 2022). Plastic fragments with less than 1000 nm are usually defined as nanoplastics (NPs) that are a

* Corresponding author at: College of Environment Science, Liaoning University, Chongshan Central Road, Shenyang, Liaoning Province, China.
E-mail address: wangzichao10@sina.com (Z. Wang).

https://doi.org/10.1016/j.biortech.2022.127627
Received 24 May 2022; Received in revised form 6 July 2022; Accepted 12 July 2022
Available online 16 July 2022

kind of emerging pollutants (Hartmann et al., 2019). Conventional wastewater treatment plants (WWTPs) have been found as a large source of NPs in natural environments, as WWTPs could hold plastics with a large size and discharge little-sized plastics (Cheung and Fok, 2017). Due to NPs with a large specific area, NPs have extraordinary adsorption abilities for chemicals from wastewaters in WWTPs (Xiong et al., 2020). This means when wastewaters contain toxic contaminants, their toxicities to bacteria may be altered due to the adsorption of toxic contaminants by NPs. Therefore, it is essential to examine the impact of polytetrafluoroethylene nanoplastics (PTFE-NPs) on the inhibition of toxic contaminants on the biological wastewater treatment performance.

Antibiotics and heavy metals are typical emerging and conventional toxic pollutants, respectively, and they have been constantly found simultaneously in WWTPs (Khurana et al., 2021). Many literatures have testified the joint influence of antibiotics and heavy metals on the biological wastewater treatment performance and found the antibiotics and heavy metals interaction resulted in the difference between the inhibition of blended antibiotics/heavy metals on bacteria and the toxicity sum of individual antibiotics and heavy metals (Khurana et al., 2021; Wang et al., 2020a; Wang et al., 2018). Notably, the interfacial interaction between NPs and antibiotics and between NPs and heavy metals contains both electrosorption (Xiong et al., 2020), implying that there would be a competitive or synergistic relationship between antibiotics and heavy metals when NPs bind with antibiotics and heavy metals (Wang et al., 2020b). Some literatures have depicted the relationship of plastic particles with antibiotics and heavy metals. Zhou et al. (2022) explored the adsorption behavior of bivalent copper (Cu(II)) on aged microplastics (average diameter 75 μm) in a binary ciprofloxacin (CIP) and Cu(II) system, and found CIP affected negatively the adsorption of Cu(II) by aged microplastics. Yu et al. (2020) stated the adsorption of Cu (II) and levofloxacin on various size microplastics (diameter ranging from 1 to 125 μm), and found that Cu(II) obviously promoted the adsorption of levofloxacin by microplastics. The biotoxicity of antibiotics and heavy metals is closely related to their free-state levels (Wang et al., 2018). This suggests that the reciprocity of microplastics with antibiotics or heavy metals would change the blended antibiotics and heavy metals toxicity to bacteria, and then alter the combined influence of antibiotics and heavy metals on the biological wastewater treatment performance. Notably, NPs are more likely to enter cells and even change cell membrane permeability due to a smaller particle size in contrast with microplastics (Alimi et al., 2018; Wei et al., 2020), which would result in a more complex potential effect of NPs on the combined toxicity of antibiotics and heavy metals to biological wastewater treatment performances. Nevertheless, the current studies only focus on the adsorption behavior of antibiotics and heavy metals on microplastics, and no information has been implemented to explore the effect of this adsorption behavior of NPs on the combined inhibition of antibiotics and heavy metals on biological wastewater treatment systems.

In the study, PTFE-NPs, CIP and Cu(II) were chose as the representative of NPs, antibiotics and heavy metals, respectively, in order (a) to assess the combined CIP and Cu(II) inhibition on the nitrogen elimination, nitrifying and denitrifying activity, extracellular polymeric substances (EPS), microbial community and interplay of sludge with CIP and/or Cu(II) in a sequencing batch reactor (SBR) with or without PTFE-NPs, and (b) to discuss the adsorption kinetics and thermodynamics of CIP and/or Cu(II) by PTFE-NPs in solutions.

2. Materials and methods

2.1. Reactors and wastewaters

Six SBRs (R1, R2, R3, R4, R5 and R6) with 50 % volume exchange rate, 7.7 L available volume, 50 cm working height and 14 cm internal diameter were set up. Every SBR in a cycle was managed according to 0.05 h influent, 5.5 h aerobic step, 1.5 h anoxic step, 0.9 h deposition and 0.05 h effluent, and the six SBRs were manipulated three cycles in one day. The dissolved oxygen in aerobic step was higher than 2.0 mg L^{-1}. Seeding sludge (R0) in the six SBRs was gained from a SBR manipulated for 30 days at no Cu(II), CIP and PTFE-NPs addition, and the average chemical oxygen demand (COD) and ammonia nitrogen (NH_4^+-N) elimination efficiencies in seeding sludge were 89.06 % and 81.31 %, respectively. The initial content of seeding sludge (measured by mixed liquor suspended sludge (MLSS)) in the six SBRs was about 4000 mg L^{-1}. The artificial wastewaters pumped into R1, R2, R3, R4, R5 and R6 contained about 400 mg L^{-1} COD, 40 mg L^{-1} NH_4^+-N and 10 mg L^{-1} phosphorus, and different levels of PTFE-NPs (average diameter 800 nm), Cu(II) and/or CIP. The influent PTFE-NPs, Cu(II) and CIP levels in the six SBRs were listed (see supplementary material).

2.2. Determining methods

The NH_4^+-N, nitrite nitrogen (NO_2^--N), nitrate nitrogen (NO_3^--N), COD, Cu(II), MLSS, and mixed liquor volatile suspended solids (MLVSS) were determined according to Wang et al. (2020a). CIP was checked in accordance with Ma et al. (2022). Specific ammonia oxidation rate (SAOR), specific nitrite oxidation rate (SNOR) and specific nitrate reduction rate (SNRR) were tested according to Wang et al. (2015). Bacterial community was detected by Personalbio Company (Shanghai, China) using a high-throughput sequencing (Wang et al., 2020a), and raw sequences data was submitted to the National Center for Biotechnology Information database (accession number: PRJNA855154). Tightly bound-EPS (TB-EPS) and loosely bound-EPS (LB-EPS) were obtained according as Wang et al. (2013). Protein (PN) and polysaccharide (PS) levels were estimated according to Lowry method (Frølund et al., 1995) and to anthrone-sulfuric acid method (Dubois et al., 1956), respectively.

2.3. Batch adsorption kinetic and thermodynamic experiments

The batch adsorption kinetic and thermodynamic experiments with Cu(II) and/or CIP by PTFE-NPs were set in a thermostatic shaker at 200 revolutions per minute, and the adsorption processes were evaluated for 18 h. The adsorption kinetics was carried out at 288 K, and the temperatures in the adsorption thermodynamic experiments were 288, 298 and 308 K, respectively. In the adsorption kinetic and thermodynamic experiments of Cu(II) and/or CIP on PTFE-NPs, the initial PTFE-NPs, Cu (II), CIP and mixed Cu(II)/CIP concentration was 1000 mg L^{-1} (to ensure that the PTFE-NPs was enough in the adsorption of CIP and Cu(II) by PTFE-NPs), 35 mg L^{-1}, 15 mg L^{-1} and 35 mg L^{-1} + 15 mg L^{-1}, respectively.

The adsorption amount was appraised by equations (eq.) (1) (Yilimulati et al., 2021).

$$q_e = \frac{(C_o - C_e) \times V}{m} \tag{1}$$

where q_e (mg g^{-1}) was the adsorbent amount at equilibrium; V (L) was the adsorption solution volume; C_0 and C_e (mg L^{-1}) were the solute levels at initial and equilibrium steps, respectively; m (g) was the PTFE-NPs amount.

Adsorption kinetics of Cu(II) and/or CIP by PTFE-NPs were assessed by the pseudo-first-order (PFO) and pseudo-second-order (PSO) adsorption kinetic models, and they were shown in eq. (2) and (3), respectively (Li et al., 2017).

$$q_t = q_{e,1}\left(1 - e^{-k_1 t}\right) \tag{2}$$

$$q_t = \frac{q_{e,2}^2 k_2 t}{1 + q_{e,2} k_2 t} \tag{3}$$

where q_t (mg g^{-1}) was adsorption capacity at time t; $q_{e,1}$ and $q_{e,2}$ (mg g^{-1}) were adsorbed amounts at equilibrium in PFO and PSO equations, respectively; k_1 (h^{-1}) and k_2 (g $mg^{-1}h^{-1}$) were adsorption rates in PFO

and PSO equations, respectively.

The adsorption thermodynamics were analyzed based on the data obtained at varying temperatures, and thermodynamic parameters were appraised by means of eq. (4), (5) and (6) (Yu et al., 2020).

$$\ln(K_d) = \frac{\Delta s}{R} - \frac{\Delta H}{RT} \quad (4)$$

$$\Delta G = -RT\ln(K_d) \quad (5)$$

$$k_d = \frac{q_e}{C_e} \quad (6)$$

where K_d was the adsorption constant of linear isotherm indicated the adsorption capacity, and its determination was according to Yilimulati et al. (2021); q_e and C_e were the same as those in eq. (1); R (8.314 J mol^{-1} K^{-1}) was the ideal gas constant at standard temperature and standard pressure; T (K) was the absolute temperature; ΔG (kJ/mol) was the free energy variation; ΔH (kJ/mol) was the enthalpy variation; ΔS (kJ/mol) was the entropy variation.

2.4. Antagonism degree index

The degree index of antagonism was used to reflect the antagonistic degree between the mixed toxic substances in the study, and the antagonistic degree index was calculated using the following equation.

$$D_t = 1 - \frac{D_{mixed}}{D_1 + D_2} \quad (7)$$

where D_t was the antagonistic degree index; D_{mixed} (%) was the decreased degree of sludge activities at the mixed toxic substances stress compared to control without toxic substances; D_1 and D_2 (%) were the decreased degree of sludge activities at the alone toxic substance 1 stress and at the alone toxic substance 2 stress, respectively, compared to control without toxic substances. D_t was defined that it ranged from 0 to 1. The larger its value was, the antagonistic effect was more obvious.

2.5. Statistical analysis

An analysis of one-way variance with Tukey test was used to assess data, and p less than 0.05 was regarded as a statistical significance. The sample analyses were performed in triplicate, and data was exhibited as means ± standard deviation.

3. Results and discussion

3.1. Performance

Fig. 1 shows the effect of PTFE-NPs on the combined inhibition of Cu (II) and CIP on COD and nitrogen removals in SBRs. At the single pressure of Cu(II) and CIP, the average COD and NH_4^+-N elimination rates were 75.81 % and 75.17 % as well as 76.40 % and 46.48 %, corresponding to R1 and R2, respectively. At the binary Cu(II) and CIP stresses, the average COD and NH_4^+-N elimination efficiencies in R3 showed 73.04 % and 38.61 %, respectively. The average COD and NH_4^+-N elimination efficiencies in R3 were always lower than those from R1 and R2, which was pertinent to the synergism or antagonism between heavy metals and antibiotics (Wang et al., 2020a; Wang et al., 2018). To reflect the effect of PTFE-NPs on the combined inhibition of Cu(II) and CIP on the COD and NH_4^+-N removals, the average elimination rates of COD and NH_4^+-N in R4, R5 and R6 with PTFE-NPs were assessed, and they were 78.37 % and 80.17 %, 71.57 % and 43.92 % as well as 66.51 % and 46.34 %, corresponding to R4, R5 and R6, respectively. The decreases in the average COD removal rate from R6 were always higher

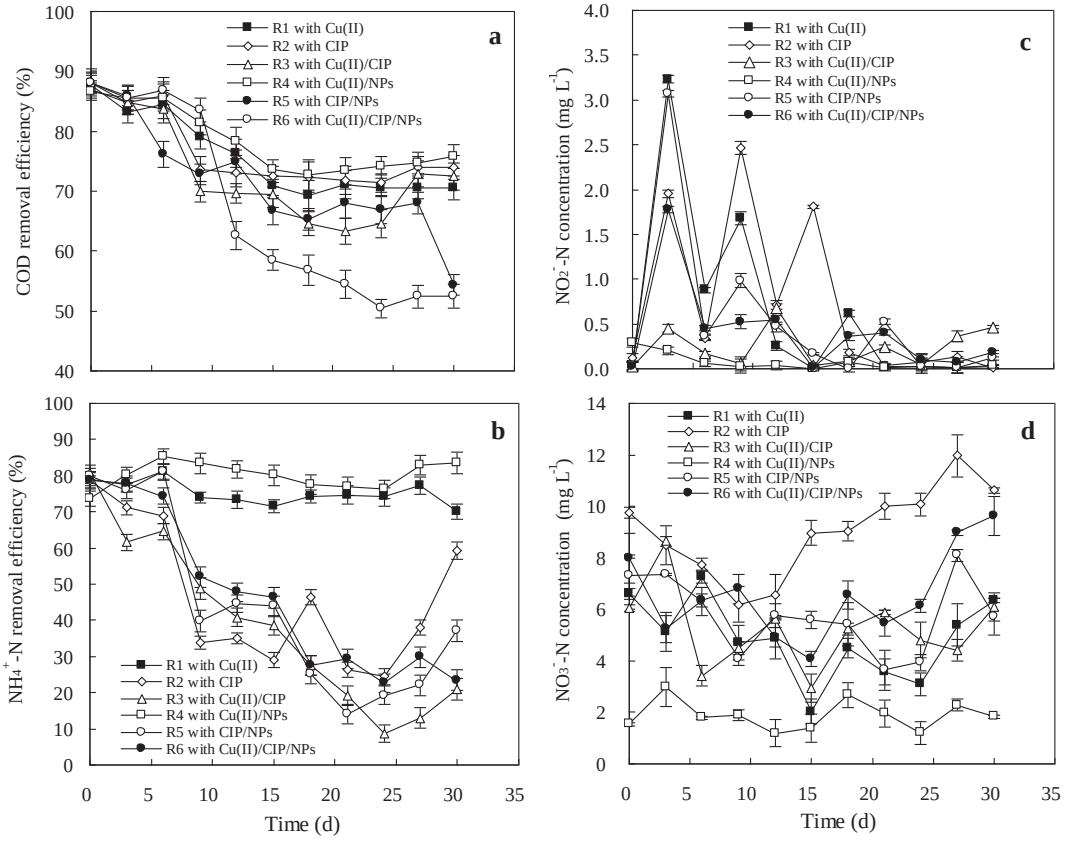

Fig. 1. Effect of PTFE-NPs on the combined inhibition of Cu(II) and CIP on COD and nitrogen removals in SBRs. (a) COD, (b) NH_4^+-N, (c) NO_2^--N, (d) NO_3^--N.

than that from R4 and R5, while the average NH_4^+-N elimination rate in R6 was less than that in R4 and was higher than that in R5. The changes on the combined inhibition of Cu(II) and CIP on the COD and NH_4^+-N elimination at the PTFE-NPs intervention were different from those without the PTFE-NPs stress. NPs could adsorb heavy metals and antibiotics (Yu et al., 2019), which could change the bioavailability of Cu(II) and CIP. In addition, NPs was also significant carriers for the heavy metals and antibiotics transport (Shen et al., 2019). These might cause that once NPs-contaminant complexes were ingested by cells, these contaminants might be simultaneously taken by cells through the NPs desorption etc.. The interaction of PTFE-NPs with Cu(II) and CIP explained why the organic and nitrogen removals with or without PTFE-NPs were different. The average effluent NO_3^--N levels in R1, R2, R3, R4, R5 and R6 were 4.87, 9.04, 5.24, 1.89, 5.75 and 6.56 mg L^{-1}, respectively. The average effluent NO_3^--N level in R3 was lower than in R2 while higher than in R1. In R6, the average effluent NO_3^--N level was always higher than in R4 and R5. Results suggested the PTFE-NPs stress changed the combined effect of Cu(II) and CIP on the NO_3^--N elimination. The effluent NO_2^--N accumulation in R1, R2, R3, R4, R5 and R6 was not constantly acquired.

3.2. Sludge activities

Fig. 2 depicts the effect of PTFE-NPs on the combined inhibition of Cu(II) and CIP on SAOR, SNOR and SNRR. The R0 sample was taken from seeding sludge at no Cu(II), CIP and PTFE-NPs. In R0, R1, R2, R3, R4, R5 and R6, the SAOR values were 14.76, 7.86, 7.81, 7.02, 11.76, 5.20 and 4.99 mg N g^{-1} VSS h^{-1}, respectively, and the SNOR values were 14.82, 7.58, 4.61, 5.92, 10.53, 6.77 and 4.41 mg N g^{-1} VSS h^{-1}, respectively. In contrast with R0, the SAOR and SNOR values in R1, R2 and R3 were reduced by 46.73 % and 48.86 %, 47.12 % and 68.93 % as well as 52.56 % and 60.08 %, respectively. The decreased degree of SAOR (or SNOR) value in R3 was less than the total SAOR (or SNOR) value decreased degree in R1 and R2, suggesting an antagonism between Cu(II) and CIP on ammonia-oxidizing bacteria (AOB) activities and nitrite-oxidizing bacteria (NOB) activities. Metal ions and antibiotics with electron-donor groups could form metals-antibiotics complexes, and they were easily absorbed by activated sludge to form metals-antibiotics-sludge complexes (Li et al., 2020a; Li et al., 2020b). This could decrease the biological availability of metals and antibiotics, which was one of reasons for the antagonistic effect of Cu(II) and CIP on the nitrifying activities of sludge. The decreased degrees of SNOR values in R1, R2 and R3 showed higher in contrast with SAOR, implying NOB

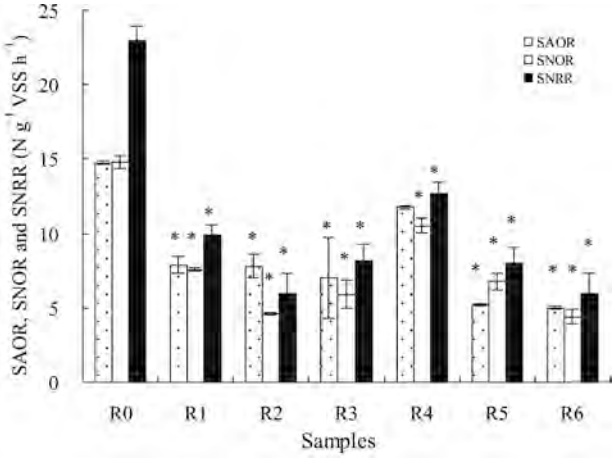

Fig. 2. Effect of PTFE-NPs on the combined inhibition of Cu(II) and CIP on SAOR, SNOR and SNRR. R0: seeding sludge. R1: with Cu(II). R2: with CIP. R3: with Cu(II)/CIP. R4: with Cu(II)/NPs. R5: with CIP/NPs. R6: with Cu(II)/CIP/NPs.

was more impressible to Cu(II) and/or CIP than AOB. The results were similar to previous study in which NOB was more sensitive to a harsh environment than AOB (Shi et al., 2021). The SAOR and SNOR values in R4, R5 and R6 at a PTFE-NPs stress were decreased by 20.36 % and 28.96 %, 64.76 % and 54.35 % as well as 66.12 % and 70.24 %, respectively, compared to R0. There was a lower decreased degree of SAOR (or SNOR) value in R6 than the sum of SAOR (or SNOR) value decreased degree in R4 and R5, suggesting no change of Cu(II) and CIP antagonistic effect on AOB and NOB was caused by PTFE-NPs. The decreased degrees of SNOR values in R4 and R6 were higher than SAOR, while the opposite result was found in R5. This suggested PTFE-NPs changed the sensitivity of AOB and NOB to CIP, and did not change those to Cu(II) and mixed Cu(II)/CIP. Li et al. (2020a), Li et al. (2020b) found that plastic particles had a significant effect on ammonia oxidation but no nitrite oxidation. The CIP concentration was the lowest among Cu(II), CIP and mixed Cu(II)/CIP, which might cause that the PTFE-NPs stress more easily affected the CIP toxicity than Cu(II) or mixed Cu(II)/CIP. In addition, the adsorption of CIP and/or Cu(II) by PTFE-NPs belonged to physical adsorption, as ΔH value in 3.4.2 section was lower than 40 kJ·mol^{-1} (Li et al., 2010). The ΔH value for CIP was the highest among Cu(II), CIP and mixed Cu(II)/CIP, suggesting that physical adsorption might had less contribution to the adsorption of PTFE-NPs for CIP than for Cu(II) or mixed Cu(II)/CIP (Chen et al., 2021). Generally, desorption was more easily found in physical adsorption (Liu et al., 2022), suggesting there might be a more obvious desorption for Cu (II) or mixed Cu(II)/CIP than for CIP. This might explain why the PTFE-NPs addition did not more obviously change the toxicity of Cu(II) or mixed Cu(II)/CIP for SAOR and SNOR than for CIP. In R0, R1, R2, R3, R4, R5 and R6, the SNRR values were 22.95, 9.88, 5.95, 8.14, 12.67, 7.97 and 5.99 mg N g^{-1} VSS h^{-1}, respectively. Compared to R0, the SNRR values without the PTFE-NPs stress in R1, R2 and R3 were reduced by 56.95 %, 74.08 % and 64.53 %, respectively, and at the PTFE-NPs stress, the SNRR values in R4, R5 and R6 were decreased by 44.77 %, 65.25 % and 73.89 %, respectively. The sum of SNRR value decreased degree in R1 and R2 and the sum from R4 and R5 were higher than the decreased degree of SNRR value in R3 and R6, respectively. The results suggested a Cu(II) and CIP antagonism on denitrifying bacteria with or without the PTFE-NPs stress. Gao et al. (2022) found that the inhibitory effect of antibiotics and heavy metals on denitrifying bacteria was antagonistic. Among R1, R2 and R3, the decreased level of SAOR in R1 showed higher than in R2 and R3, while the SNOR and SNRR decreased levels in R1 showed less than in R2 and more than in R3. Differently, the SAOR, SNOR and SNRR decreased levels in R6 were always higher than in R4 and R5. The changes showed an increase in the mixed Cu(II)/CIP inhibition on SAOR, SNOR and SNRR as the PTFE-NPs addition, suggesting that the Cu(II) and CIP antagonism to nitrifiers and denitrifiers was weakened by the PTFE-NPs intervention.

To further assess the influence of PTFE-NPs on the Cu(II) and CIP antagonistic effect on SAOR, SNOR and SNRR, the antagonism degree index (*Dt*) was calculated, and the results were shown in Fig. 3. The larger *Dt* value was, the interaction between mixtures more easily affected their toxicities to SAOR, SNOR and SNRR. The *Dt* values for SAOR, SNOR and SNRR at no PTFE-NPs stress were 0.44, 0.49 and 0.51, respectively, implying the Cu(II) and CIP interaction at no PTFE-NPs had more distinct effects on denitrifiers than nitrifiers, and on NOB than AOB. At the PTFE-NPs stress, the *Dt* values for SAOR, SNOR and SNRR were 0.22, 0.16 and 0.33, respectively. The *Dt* values with PTFE-NPs were always lower than at no PTFE-NPs, suggesting the PTFE-NPs stress increased the influence of CIP and Cu(II) interaction on nitrifying and denitrifying activities. NPs could increase bacterial permeability (Feng et al., 2020a), resulting in the entry of more Cu(II) and/or CIP into cells at PTFE-NPs stress. Additionally, the synergistic adsorption of CIP and Cu(II) by PTFE-NPs and their desorption could be found based on the analyses of adsorption kinetics and thermodynamics, respectively (3.4.2 section), meaning when PTFE-NPs were ingested by cells, CIP and Cu(II) could also be simultaneously taken by cells (Shen et al., 2019).

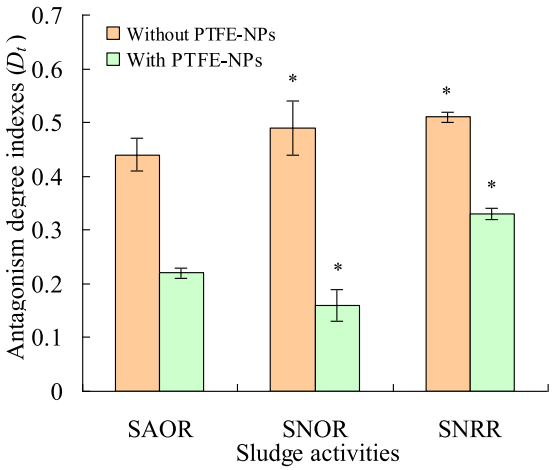

Fig. 3. The antagonism degree indexes between Cu(II) and CIP on SAOR, SNOR and SNRR with or without PTFE-NPs.

These could also cause more CIP and Cu(II) to enter into cells, and resulted in the increase in the mixed Cu(II)/CIP breach to cells with PTFE-NPs compared to no PTFE-NPs. These could interpret why the *Dt* values for SAOR, SNOR and SNRR at PTFE-NPs stress were lower than at no PTFE-NPs. At no PTFE-NPs, the *Dt* value for SNOR was higher than SAOR and lower than SNRR, while under PTFE-NPs stress, the *Dt* value for SNOR was the lowest among SAOR, SNOR and SNRR. Results implied the Cu(II) and CIP antagonism on SNOR was most distinctly changed by PTFE-NPs among SAOR, SNOR and SNRR. The changing trend of *Dt* values for SAOR, SNOR and SNRR with and without PTFE-NPs were different, which might be pertinent to the PTFE-NPs biotoxicity. This need to be studied future.

3.3. Microbial community

Fig. 4a shows the impacts of PTFE-NPs on the joint Cu(II) and CIP inhibition on the evolutions of functional bacterial community involved in nitrification and denitrification at the genus level. There were about 200 recognized genera that their mean relative abundance in the seven samples was always more than 0.01 %, and the genus composition changes were analyzed based on 50 genera with more than 95 % of total abundance. In the 50 genera, 14 genera pertained to nitrifers and denitrifers. The genera *Nitrosomonas* and *Nitrospira* pertained to nitrifying bacteria (Yang et al., 2021), and these genera *Nitratireductor*, *Caulobacter*, *Reyranella*, *Acidovorax*, *Cupriavidus*, *Dechloromonas*, *Denitratisoma*, *Leptothrix*, *Thauera*, *Thiomonas*, *Pseudomonas* and *Comamonas* belonged to denitrifying bacteria (Feng et al., 2020b; Wang et al., 2020a; Xia et al., 2019). The effect of PTFE-NPs on the nitrifiers and denitrifiers relative levels and their changed degrees at the Cu(II) and/or CIP stress are depicted in Fig. 4b and 4c. In R0 (seeding sludge), R1, R2 and R3, the denitrifers relative level was 75.60 %, 65.79 %, 44.83 % and 60.22 %, respectively, and compared to R0, the decreased degrees in R1, R2 and R3 showed 12.97 %, 40.70 % and 20.34 %, respectively. The sum of denitrifers relative abundance reduced level in R1 and R2 was 53.67 %, which was higher than R3. Results might lead to the Cu(II) and CIP

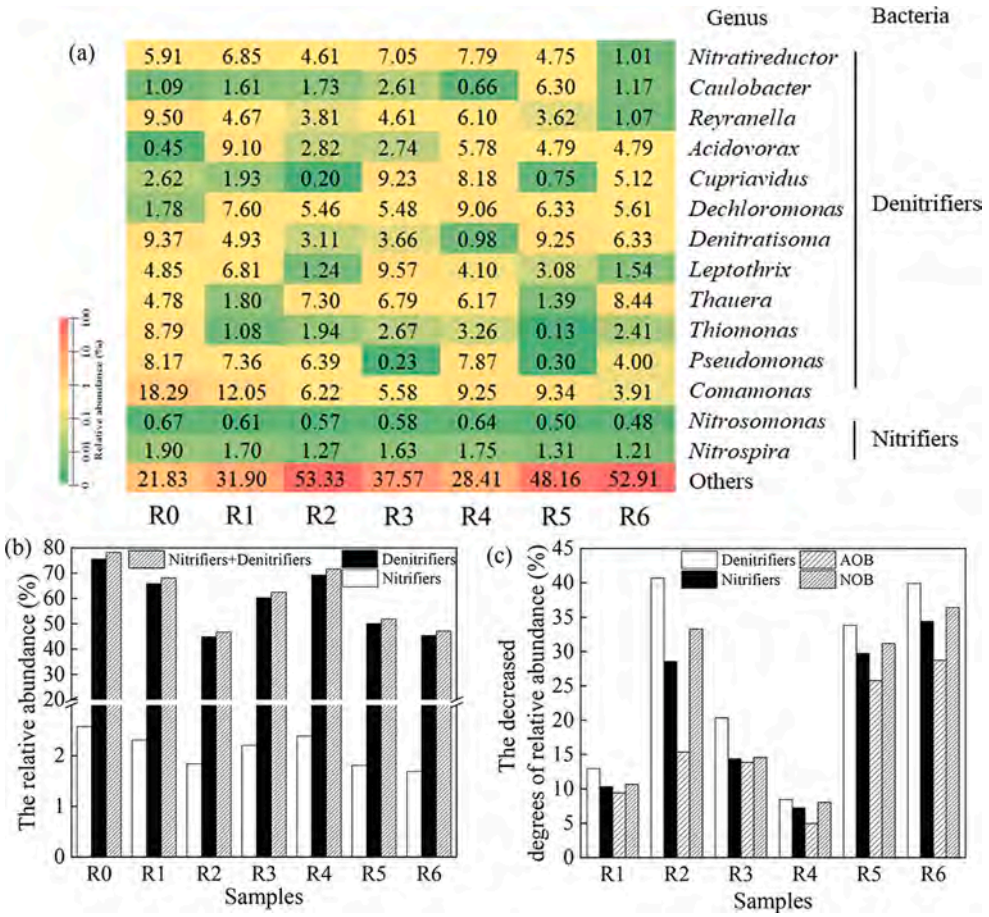

Fig. 4. Effect of PTFE-NPs on the combined inhibition of Cu(II) and CIP on (a) the evolutions of functional microbial community associated with nitrification and denitrification, (b) the total relative abundance of nitrifiers (or denitrifiers) and (c) the decreased degrees of relative abundance of nitrifiers, denitrifiers, AOB and NOB at the genus level. R0: seeding sludge. R1: with Cu(II). R2: with CIP. R3: with Cu(II)/CIP. R4: with Cu(II)/NPs. R5: CIP/NPs. R6: with Cu(II)/CIP/NPs.

antagonistic effect on SNRR. This was similar to previous studies in which zinc and tetracycline antagonistically affected the activities of nitrate and nitrite reductase (Wang et al., 2020a). The denitrifers relative abundance in R4, R5 and R6 was 69.20 %, 50.03 % and 45.40 %, respectively, and compared to R0, the reduced degrees in R4, R5 and R6 were 8.46 %, 33.82 % and 39.94 %, respectively. The sum of denitrifers relative abundance decreased degree in R4 and R5 was 42.28 %, which was higher than R6. The changes suggested there was still a Cu(II) and CIP antagonistic effect on SNRR under a PTFE-NPs stress. The decreased degree of denitrifers relative level in R6 showed higher than in R4 and R5. While the decreased degree was more in R3 than in R1 and lower than in R2. Results suggested the PTFE-NPs stress increased the inhibition of mixed Cu(II) and CIP on denitrifiers compared to no PTFE-NPs. This might decrease the antagonistic effect between Cu(II) and CIP on SNRR at a PTFE-NPs stress compared to no PTFE-NPs.

Similarly, in R0, R1, R2, R3, R4, R5 and R6, the genus *Nitrosomonas* relative abundance was 0.67 %, 0.61 %, 0.57 %, 0.58 %, 0.64 %, 0.50 % and 0.48 %, respectively, and the genus *Nitrospira* relative level showed 1.90 %, 1.70 %, 1.27 %, 1.63 %, 1.75 %, 1.31 % and 1.21 %, respectively. Compared to R0, the genus *Nitrosomonas* relative abundance reduced levels in R1, R2, R3, R4, R5 and R6 were 9.42 %, 15.36 %, 13.87 %, 4.96 %, 25.75 % and 28.72 %, respectively, and the genus *Nitrospira* relative abundance decreased levels were 10.67 %, 33.26 %, 14.57 %, 8.04 %, 31.16 % and 36.42 %, respectively. The sum of genera *Nitrosomonas* and *Nitrospira* relative level decreased degree in R1 and R2 was 24.78 % and 43.93 %, respectively, and they were always higher than the genera *Nitrosomonas* and *Nitrospira* relative abundance in R3. The changes could result in the Cu(II) and CIP antagonistic effect on SAOR and SNOR. Analogously, the genus *Nitrosomonas* (or *Nitrospira*) relative abundance in R6 was lower than the sum of genus *Nitrosomonas* (or *Nitrospira*) relative abundance decreased degree in R4 and R5. At a PTFE-NPs stress, the decreased degrees of genera *Nitrosomonas* and *Nitrospira* relative abundance with mixed Cu(II)/CIP were closer to their sum with alone Cu(II) and CIP, compared to no PTFE-NPs stress. The results might cause the Cu(II) and CIP antagonistic effect on SAOR and SNOR at no PTFE-NPs stress was more obvious than that with PTFE-NPs. The decreased degree of denitrifiers in R1, R2, R3, R4, R5 and R6 was always higher than nitrifiers, and the decreased degree of genus *Nitrospira* was higher than the genus *Nitrosomonas*. The results suggested with or without PTFE-NPs, Cu(II) and/or CIP always had a distinct impact on denitrifiers than nitrifiers, and on the genus *Nitrospira* than the genus *Nitrosomonas*.

3.4. Adsorption behavior

To understand the effect of PTFE-NPs on the Cu(II) and CIP antagonism on sludge activities, the adsorption kinetics and thermodynamics were investigated.

3.4.1. Adsorption kinetics

Fig. 5 shows the single and binary adsorption processes of CIP and Cu (II) by PTFE-NPs. The single system was the adsorption of CIP or Cu(II) by PTFE-NPs, while the binary system was the adsorption of PTFE-NPs with CIP and Cu(II). The rapid increase in the adsorption amount (q_t) of PTFE-NPs for CIP and Cu(II) in the single and binary system could be found in the initial phase, and then the increase gradually slowed. The changes suggested that the adsorption of PTFE-NPs with CIP and Cu(II) occurred on the surface of PTFE-NPs (Yu et al., 2020). When q_t for CIP and/or Cu(II) in the single and binary system was not obviously altered as time, the adsorption equilibrium was achieved. The q_t value under the adsorption equilibrium condition was regarded as the max adsorption amount. The max adsorption amounts for CIP by PTFE-NPs in the single and binary systems were 1.01 and 1.28 mg g^{-1}, respectively, and the max Cu(II) adsorption amounts of PTFE-NPs were 0.85 and 0.89 mg g^{-1}, respectively, corresponding to the single system and the binary system. Xue et al. (2021) reported similar results in which antibiotics were

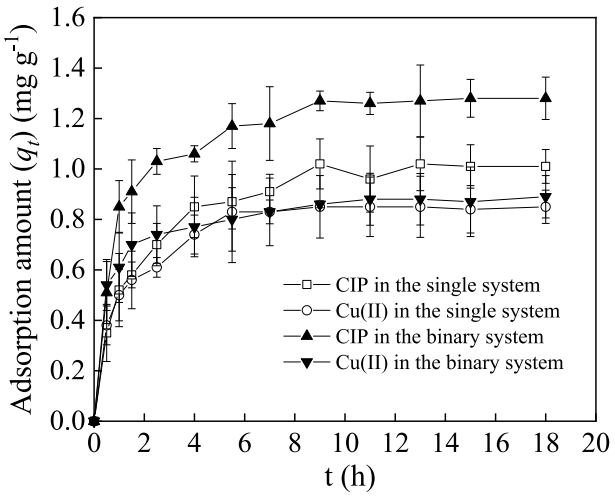

Fig. 5. The single and binary adsorption processes of CIP and Cu(II) by PTFE-NPs.

adsorbed by microplastics more easily than metals whether in the single or binary systems of antibiotics and metals. The max adsorption amounts for CIP and Cu(II) by PTFE-NPs were always higher in the binary system than in the single system, suggesting a synergistic adsorption process between CIP and Cu(II) by PTFE-NPs. The results were coincident with previous literatures in which the synergistic adsorption was due to the complex of carboxyl/amino group from antibiotics to metal ions (Chen and Li, 2022). As the desorption of PTFE-NPs with CIP and Cu(II) was achieved (see 3.4.2 section), the synergistic adsorption process of CIP and Cu(II) by PTFE-NPs might cause more CIP and Cu(II) in cells were found in the binary system after the adsorption of PTFE-NPs by cells than the single system. More entry of CIP and Cu(II) into cells through the synergistic transport of PTFE-NPs could explain why the combined CIP and Cu(II) toxicity to bacteria was increased by the stress of PTFE-NPs. The CIP and Cu(II) complexes toxicity to bacteria showed less than alone Cu(II) and was higher than individual CIP (Zhang et al., 2012). This might be one of reasons the combined CIP and Cu(II) toxicity to bacteria at a PTFE-NPs stress was still antagonistic. To understand the mass transfer process of CIP and Cu(II) by PTFE-NPs in the single and binary systems, the adsorption kinetics was analyzed using the pseudo-first-order (PFO) model and the pseudo-second-order (PSO) model, and the fitting properties are depicted (see supplementary material). The correlation coefficient (R^2) values for the PFO model and the PSO model were always higher than 0.95 in the single and binary systems, revealing both the PFO model and the PSO model could match the data well. The evolutions suggested the mass transfer processes of CIP and Cu(II) by PTFE-NPs in the single and binary systems were both dependent on the sorbent concentration (based on the PFO model fitting results) and the available sorption domains of PTFE-NPs (based on the PSO model fit results) (Yao et al., 2021). For the PFO model, the adsorption reaction rates (k_1) of Cu(II) and CIP on PTFE-NPs in the single system were 0.80 and 0.62 h^{-1}, respectively, and those in the binary system were 1.53 and 1.98 h^{-1}, respectively. Similarly, for the PSO model, the adsorption reaction rates (k_2) of Cu(II) and CIP on PTFE-NPs in the single system were 0.91 and 0.77 h^{-1}, respectively, and those in the binary system were 2.86 and 1.05 h^{-1}, respectively. The adsorption reaction rates of Cu(II) or CIP on PTFE-NPs in the single systems were always lower than those in the binary systems, suggesting binary Cu(II) and CIP promoted their adsorptions by PTFE-NPs. Previous studies reported similar results in which the interaction between antibiotics and metals served as bridges increased the adsorptivity of plastic particles with antibiotics (or metals) to metals (or antibiotics) (Yu et al., 2020; Zhou et al., 2022).

3.4.2. Adsorption thermodynamics

To understand the dynamic forces of CIP and/or Cu(II) adsorption on PTFE-NPs, the adsorption thermodynamics were analyzed in the single and binary systems, and the ΔG, ΔH and ΔS values are shown (see supplementary material). In the single CIP or Cu(II) adsorption process by PTFE-NPs at 288, 298 and 308 K, the ΔG values for the CIP adsorption on PTFE-NPs showed 5.30, 5.07 and 4.83 kJ·mol^{-1}, respectively, and they in the Cu(II) adsorption by PTFE-NPs were 5.70, 5.73 and 5.76 kJ·mol^{-1}, respectively. Similarly, in the binary CIP and Cu(II) adsorption system by PTFE-NPs, the ΔG values for CIP at 288, 298 and 308 K were 4.61, 4.53 and 4.44 kJ·mol^{-1}, respectively, and were 5.60, 5.56 and 5.52 kJ·mol^{-1} for Cu(II), respectively. The ΔG values in the single system showed higher than those in the binary system, implying the binary Cu(II) and CIP promoted their adsorptions by PTFE-NPs. The results were similar to Xue et al. (2021) in which higher ΔG values in the single adsorption of Cu(II) or oxytetracycline by thermoplastic polyurethane microplastics were found compared to their binary adsorption system. The ΔG values at different temperatures in the single and binary system were always positive, suggesting the adsorption process of CIP and/or Cu(II) by PTFE-NPs was nonspontaneous, and the complex of PTFE-NPs with CIP and/or Cu(II) was not stable (Guo et al., 2022). The results were similar to previous studies, in which the adsorption of antibiotics on microplastics was nonspontaneous, and the adsorption was promoted by vibration (Yu et al., 2020). The ΔH values for CIP and Cu (II) in the single system were 12.05 and 4.92 kJ·mol^{-1}, respectively, and they in the binary system were 7.06 and 6.72 kJ·mol^{-1}, respectively. Chen et al. (2021) found that physical adsorption played a dominant role when ΔH was less than 40 kJ·mol^{-1}. Generally, physical adsorption had lower stability than chemical adsorption (Liu et al., 2022). This was one of the reasons that the complex of PTFE-NPs with CIP and/or Cu(II) was not stable. The ΔS changes could reveal whether the adsorption process involved in an associative or dissociative mechanism, and the ΔS value above −10 kJ·mol^{-1} meant the adsorption conformed to a dissociative mechanism (Akpomie et al., 2015). The ΔS values in the single and binary system for CIP were 23.44 and 8.51 kJ·mol^{-1}, respectively, and they for Cu(II) were −2.73 and 3.91 kJ·mol^{-1}, respectively. The ΔS values in the single and binary system for CIP and Cu(II) were always higher than −10 kJ·mol^{-1}, which also confirmed CIP and/or Cu(II) could be desorbed from the unstable PTFE-NPs complex with CIP and Cu (II). Wu et al. (2019) observed the desorption of bisphenol analogues from microplastics when ΔS was larger than −10 kJ·mol^{-1}. The adsorption thermodynamics showed that the nonstable complex of PTFE-NPs with CIP and/or Cu(II) could be formatted in their adsorption processes, and the nonstable complex formation might lead to the results that more CIP and Cu(II) could enter into cells through the desorption of CIP and/or Cu(II) from the nonstable PTFE-NPs complex with CIP and Cu(II) inside cells compared to no PTFE-NPs. The changes explained why the PTFE-NPs existence decreased the antagonistically combined toxicity of CIP and Cu(II) to bacteria.

3.5. Extracellular polymeric substances

Fig. 6 shows the effect of PTFE-NPs on the joint inhibition of Cu(II) and CIP on EPS. The PN and PS contents from LB-EPS in R0, R1, R2, R3, R4, R5 and R6 were 11.87 and 1.92, 26.22 and 3.77, 24.50 and 2.03, 55.53 and 3.83, 50.10 and 3.63, 33.46 and 2.13 as well as 42.14 and 2.40 mg g^{-1} VSS, respectively, and those from TB-EPS showed 16.83 and 2.62, 29.13 and 3.88, 28.90 and 3.27, 58.40 and 3.75, 33.87 and 2.63, 56.85 and 4.32 as well as 50.77 and 2.78 mg g^{-1} VSS, respectively. Compared to R0, the PN and PS levels from LB-EPS and TB-EPS increased, which was related to bacterial protective responses to harmful environments (Wang et al., 2020a). The PN/PS ratios from LB-EPS and TB-EPS were 6.18 and 6.41, 6.95 and 7.51, 12.05 and 8.84, 14.51 and 13.16, 13.82 and 15.59, 15.70 and 12.86 as well as 17.59 and 18.24, respectively, corresponding to R0, R1, R2, R3, R4, R5 and R6. The PN/PS ratio in R0 showed the lowest in the seven samples, suggesting

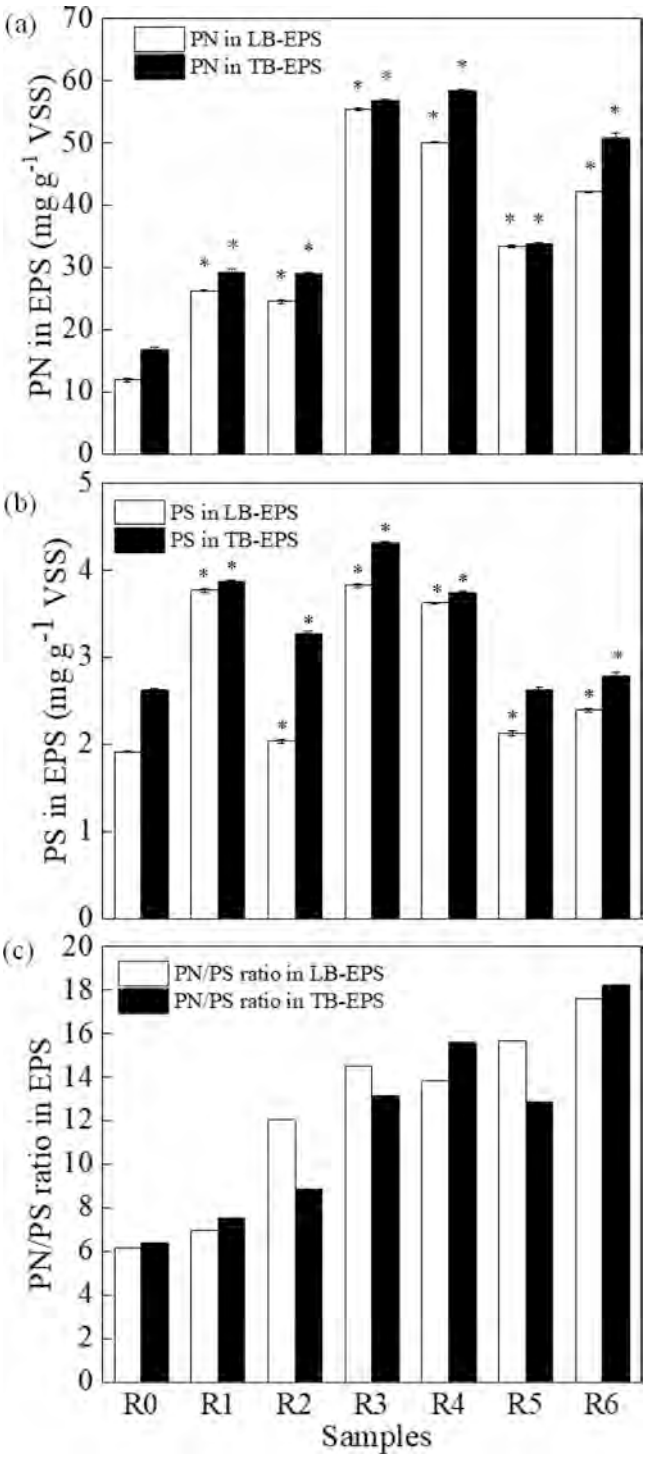

Fig. 6. Effect of PTFE-NPs on the combined inhibition of Cu(II) and CIP on (a) PN, (b) PS and (c) PN/PS ratio in EPS. R0: seeding sludge. R1: with Cu(II). R2: with CIP. R3: with Cu(II)/CIP. R4: with Cu(II)/NPs. R5: with CIP/NPs. R6: with Cu(II)/CIP/NPs.

with or without PTFE-NPs, PN had a more critical role in protecting bacteria from the toxicity of Cu(II) and/or CIP than PS. Previous studies reported similar results that bacteria secreted more PN to decrease the toxicity of metals and antibiotics to them rather than PS (Wang et al., 2017; Zheng et al., 2016). Compared to R0, the PN level from LB-EPS and TB-EPS in R1, R2 and R3 increased by 120.89 % and 73.08 %, 106.43 % and 71.72 % as well as 367.84 % and 229.96 %, respectively. The increased degree of PN from LB-EPS (or TB-EPS) in R3 was higher

than the total increased level from R1 and R2, suggesting the bacterial protective responses to the binary Cu(II) and CIP stress might be higher than the sum of protective levels to the single Cu(II) and CIP stress. The results might be one of reasons that Cu(II) and CIP had antagonistic effects on SAOR, SNOR and SNRR. The increased degree of PN from LB-EPS showed higher than TB-EPS, suggesting at no PTFE-NPs stress, PN from LB-EPS played more important roles in protecting bacteria from the single and binary stresses of Cu(II) and CIP than TB-EPS. Compared to R0, the PN content from LB-EPS and TB-EPS in R4, R5 and R6 increased by 322.03 % and 247.01 %, 181.87 % and 101.27 % as well as 255.05 % and 201.64 %, respectively. At a PTFE-NPs stress, the increased degree of PN from LB-EPS was higher than TB-EPS, which was similar to the results at no PTFE-NPs. The changes suggested with or without PTFE-NPs, PN from LB-EPS had a more critical protective role for bacteria at the single and binary stresses of Cu(II) and CIP than that from TB-EPS. This was similar to previous study in which more PN was found in LB-EPS than in TB-EPS under harmful environment (Wang et al., 2017). While at a PTFE-NPs stress, the increased degree of PN from LB-EPS (or TB-EPS) in R6 was lower than the sum of increased degree in R4 and R5, suggesting the protective role from PN of LB-EPS (or TB-EPS) in R6 might be less than the sum in R4 and R5. The results with a PTFE-NPs stress were contrary to those at no PTFE-NPs, which might explain why the PTFE-NPs stress decreased the Cu(II) and CIP antagonistic effect on SAOR, SNOR and SNRR.

4. Conclusions

The COD and NH_4^+-N removal rates decreased as the Cu(II) and/or CIP addition with or without PTFE-NPs. The PTFE-NPs addition weakened the antagonistic effect of Cu(II) and CIP on the nitrifying and denitrifying activities of sludge, and enlarged the degree of reduction in the relative level from nitrifiers and denitrifiers with mixed Cu(II)/CIP. PTFE-NPs did no change the results that denitrifiers were more impressible to Cu(II) and/or CIP than nitrifiers. Mixed Cu(II)/CIP promoted their adsorptions by PTFE-NPs based on adsorption kinetics and thermodynamics. With or without PTFE-NPs, PN had more obvious protective responses to Cu(II) and/or CIP than PS.

CRediT authorship contribution statement

Huan Yang: Methodology, Data curation. **Yueyue Wang:** Software, Methodology. **Zichao Wang:** Writing – original draft, Writing – review & editing, Funding acquisition. **Shengyu Yuan:** Methodology, Data curation. **Changwei Niu:** Investigation. **Yaohui Liu:** Investigation. **Yun Gao:** Software. **Yuhan Li:** Software. **Dan Su:** Software. **Youtao Song:** Investigation.

Declaration of Competing Interest

The authors declare that they have no known competing financial interests or personal relationships that could have appeared to influence the work reported in this paper.

Data availability

The authors do not have permission to share data.

Acknowledgements

The works were supported by the National Natural Science Foundation of China (No. 51708079); the Scientific Research Project of Liaoning Province Education Department, China (No. LJC201912); the Young Scientific and Technological Innovation Talents Project of Shenyang City, China (No. RC210057).

Appendix A. Supplementary data

Supplementary data to this article can be found online at https://doi.org/10.1016/j.biortech.2022.127627.

References

Akpomie, K.G., Dawodu, F.A., Adebowale, K.O., 2015. Mechanism on the sorption of heavy metals from binary-solution by a low cost montmorillonite and its desorption potential. Alex. Eng. J. 54, 757–767.
Alimi, O., Farner Budarz, J., Hernandez, L.M., Tufenkji, N., 2018. Microplastics and nanoplastics in aquatic environments: Aggregation, deposition, and enhanced contaminant transport. Environ. Sci. Technol. 52, 1704–1724.
Chen, Y., Li, J., Wang, F., Yang, H., Liu, L., 2021. Adsorption of tetracyclines onto polyethylene microplastics: A combined study of experiment and molecular dynamics simulation. Chemosphere 265, 129133.
Cheung, P.K., Fok, L., 2017. Characterisation of plastic microbeads in facial scrubs and their estimated emissions in Mainland China. Water Res. 122, 53–61.
Dubois, M., Gilles, K.A., Hamilton, J.K., Rebers, P.A., Smith, F., 1956. Colorimetric method for determination of sugars and related substance. Anal. Chem. 28, 350–356.
Feng, L.J., Sun, X.D., Zhu, F.P., Feng, Y., Duan, J.L., Xiao, F., Li, X.Y., Shi, Y., Wang, Q., Sun, J.W., Liu, X.Y., Liu, J.Q., Zhou, L.L., Wang, S.G., Ding, Z., Tian, H., Galloway, T. S., Yuan, X.Z., 2020b. Nanoplastics promote microcystin synthesis and release from cyanobacterial Microcystis aeruginosa. Environ. Sci. Technol. 54, 3386–3394.
Feng, L., Yang, J., Yu, H., Lan, Z., Ye, X., Yang, G., Yang, Q., Zhou, J., 2020a. Response of denitrifying community, denitrification genes and antibiotic resistance genes to oxytetracycline stress in polycaprolactone supported solid-phase denitrification reactor. Bioresour. Technol. 308, 123274.
Frølund, B., Griebe, T., Nielsen, P.H., 1995. Enzymatic activity in the activated sludge floc matrix. Appl. Microbiol. Biotechnol. 43, 755–761.
Gao, Y.X., Li, X., Fan, X.Y., Zhao, J.R., Zhang, Z.X., 2022. The dissimilarity of antibiotic and quorum sensing inhibitor on activated sludge nitrification system: Microbial communities and antibiotic resistance genes. Bioresour. Technol. 351, 127016.
Guo, X., Xu, Z., Zheng, X., Jin, X., Cai, J., 2022. Understanding pyrolysis mechanisms of corn and cotton stalks via kinetics and thermodynamics. J. Anal. Appl. Pyrolysis 164, 105521.
Hartmann, N.B., Hüffer, T., Thompson, R.C., Hassellöv, M., Verschoor, A., Daugaard, A. E., Rist, S., Karlsson, T., Brennholt, N., Cole, M., Herrling, M.P., Hess, M.C., Ivleva, N. P., Lusher, A.L., Wagner, M., 2019. Are we speaking the same language? Recommendations for a definition and categorization framework for plastic debris. Environ. Sci. Technol. 53, 1039–1047.
Karpenko, A.A., Odintsov, V.S., Istomina, A.A., 2022. Micro-nano-sized polytetrafluoroethylene (teflon) particles as a model of plastic pollution detection in living organisms. Environ. Sci. Pollut. Res. 29, 11281–11290.
Khurana, P., Pulicharla, R., Brar, S.K., 2021. Antibiotic-metal complexes in wastewaters: fate and treatment trajectory. Environ. Int. 157, 106863.
Li, L., Song, K., Yeerken, S., Geng, S., Liu, D., Dai, Z., Xie, F., Zhou, X., Wang, Q., 2020a. Effect evaluation of microplastics on activated sludge nitrification and denitrification. Sci. Total Environ. 707, 135953.
Li, Q., Yue, Q.Y., Su, Y., Gao, B.Y., Sun, H.J., 2010. Equilibrium, thermodynamics and process design to minimize adsorbent amount for the adsorption of acid dyes onto cationic polymer-loaded bentonite. Chem. Eng. J. 158, 489–497.
Li, Q., Song, W., Sun, M., Li, J., Yu, Z., 2020b. Response of *Bacillus vallismortis* sp. EPS to exogenous sulfur stress/induction and its adsorption performance on Cu(II). Chemosphere 251, 126343.
Li, S., Zhang, X., Huang, Y., 2017. Zeolitic imidazolate framework-8 derived nanoporous carbon as an effective and recyclable adsorbent for removal of ciprofloxacin antibiotics from water. J. Hazard. Mater. Adv. 321, 711–719.
Liu, W., Qiu, X., Song, Y., Zhang, X., Tian, S., Liu, L., 2022. Adsorption behavior of CF_4 and COF_2 gas on the GaN monolayer doped with Pt catalytic: A first-principles study. Surf. Sci. 719, 122032.
Ma, Y., Wang, Z., Li, J., Song, B., Liu, S., 2022. Electrochemical-assisted ultraviolet light coupled peroxodisulfate system to degrade ciprofloxacin in water: Kinetics, mechanism and pathways. Chemosphere 295, 133838.
Shen, M., Zhang, Y., Zhu, Y., Song, B., Zeng, G., Hu, D., Wen, X., Ren, X., 2019. Recent advances in toxicological research of nanoplastics in the environment: A review. Environ. Pollut. 252, 511–521.
Shi, Y.J., Yang, L., Liao, S.F., Zhang, L.G., Liao, Z.C., Lan, M.Y., Sun, F., Ying, G.G., 2021. Responses of aerobic granular sludge to fluoroquinolones: Microbial community variations, and antibiotic resistance genes. J. Hazard. Mater. 414, 125527.
Wang, X., Dai, H., Zhang, J., Yang, T., Chen, F., 2017. Unraveling the long-term effects of Cr(VI) on the performance and microbial community of nitrifying activated sludge system. Water 9, 909.
Wang, Z., Gao, M., Wang, Z., She, Z.L., Chang, Q., Sun, C., Zhang, J., Ren, Y., Yang, N., 2013. Effect of salinity on extracellular polymeric substances of activated sludge from an anoxic-aerobic sequencing batch reactor. Chemosphere 93, 2789–2795.
Wang, Z., Gao, M., Ren, Y., Wang, Z., She, Z., Jin, C., Chang, Q., Sun, C., Zhang, J., Yang, N., 2015. Effect of hydraulic retention time on performance of an anoxic–aerobic sequencing batch reactor treating saline wastewater. Int. J. Environ. Sci. Technol. 12, 2043–2054.
Wang, Y., Wang, X., Li, Y., Li, J., Wang, F., Xia, S., Zhao, J., 2020a. Biofilm alters tetracycline and copper adsorption behaviors onto polyethylene microplastics. Chem. Eng. J. 392, 123808.

Wang, Z., Xia, P., Gao, M., Ma, K., Deng, Z., Wei, J., Zhang, J., Wang, L., Zheng, G., Yang, Y., Chen, J., Wang, Y., 2018. Long-term effects of combined divalent copper and tetracycline on the performance, microbial activity and community in a sequencing batch reactor. Bioresour. Technol. 249, 916–923.

Wang, Z., Yuan, S., Deng, Z., Wang, Y., Deng, S., Song, Y., Sun, C., Bu, N., Wang, X., 2020b. Evaluating responses of nitrification and denitrification to the co-selective pressure of divalent zinc and tetracycline based on resistance genes changes. Bioresour. Technol. 314, 123769.

Wei, W., Hao, Q., Chen, Z., Bao, T., Ni, B.J., 2020. Polystyrene nanoplastics reshape the anaerobic granular sludge for recovering methane from wastewater. Water Res. 182, 116041.

Wu, P., Cai, Z., Jin, H., Tang, Y., 2019. Adsorption mechanisms of five bisphenol analogues on PVC microplastics. Sci. Total Environ. 650, 671–678.

Xia, Z., Wang, Q., She, Z., Gao, M., Zhao, Y., Guo, L., Jin, C., 2019. Nitrogen removal pathway and dynamics of microbial community with the increase of salinity in simultaneous nitrification and denitrification process. Sci. Total Environ. 697, 134047.

Xiong, Y., Zhao, J., Li, L., Wang, Y., Dai, X., Yu, F., Ma, J., 2020. Interfacial interaction between micro/nanoplastics and typical PPCPs and nanoplastics removal via electrosorption from an aqueous solution. Water Res. 184, 116100.

Xue, X.D., Fang, C.R., Zhuang, H.F., 2021. Adsorption behaviors of the pristine and aged thermoplastic polyurethane microplastics in Cu(II)-OTC coexisting system. J. Hazard. Mater. 407, 124835.

Yang, H., Wang, Z., Yuan, S., Wang, Y., Song, Y., Bu, N., Wang, L., Zhang, L., 2021. Combined impacts of diclofenac and divalent copper on the nitrogen removal, bacterial activity and community from a sequencing batch reactor. J. Water Process. Eng. 43, 102212.

Yilimulati, M., Wang, L., Ma, X., Yang, C., Habibul, N., 2021. Adsorption of ciprofloxacin to functionalized nano-sized polystyrene plastic: Kinetics, thermochemistry and toxicity. Sci. Total Environ. 750, 142370.

Yu, F., Yang, C., Zhu, Z., Bai, X., Ma, J., 2019. Adsorption behavior of organic pollutants and metals on micro/nanoplastics in the aquatic environment. Sci. Total Environ. 694, 133643.

Yu, F., Li, Y., Huang, G., Yang, C., Chen, C., Zhou, T., Zhao, Y., Ma, J., 2020. Adsorption behavior of the antibiotic levofloxacin on microplastics in the presence of different heavy metals in an aqueous solution. Chemosphere 260, 127650.

Zhang, Y., Cai, X., Lang, X., Qiao, X., Li, X., Chen, J., 2012. Insights into aquatic toxicities of the antibiotics oxytetracycline and ciprofloxacin in the presence of metal: complexation versus mixture. Environ. Pollut. 166, 48–56.

Zheng, D., Chang, Q., Li, Z., Gao, M., She, Z., Wang, X., Guo, L., Zhao, Y., Jin, C., Gao, F., 2016. Performance and microbial community of a sequencing batch biofilm reactor treating synthetic mariculture wastewater under long-term exposure to norfloxacin. Bioresour. Technol. 222, 139–147.

Zhou, Z., Sun, Y., Wang, Y., Yu, F., Ma, J., 2022. Adsorption behavior of Cu(II) and Cr(VI) on aged microplastics in antibiotics-heavy metals coexisting system. Chemosphere 291, 132794.